Proceedings of the 17th Pan-American Conference on Soil Mechanics and Geotechnical Engineering (XVII PCSMGE), and 2nd Latin-American Regional Conference of the International Association for Engineering Geology and the Environment (IAEG), La Serena Chile, 2024.

The use of Artificial Intelligence, Finite Element Modelling and Pressuremeter tests for geotechnical characterisation.

El uso de Inteligencia Artificial, Modelación con Elementos Finitos y ensayos de Presiómetro para la caracterización geotécnica.

Rafael Martínez & Maximiliano Jara
Pangea Geotecnia, Chile, Rafael.martinez@pangealtda.cl

ABSTRACT: Pressuremeter tests have been used for many years but the difficulty for interpreting its results has hindered its wide use. Nowadays, with the rise of fast computers and readily available finite element softwares the problem of interpretation can be overcome. In this manner, the test can be modelled and the soil parameters can be determined by matching the field curve with the finite element model. In this way it is possible to characterize the soil and calibrate a constitutive model in a single process. Even though the procedure appears straightforward, in practice a manual calibration can be time consuming and tedious. In order to expedite this process and obtain a close match, a novel and powerful geotechnical software (DAARWIN) that uses Artificial Intelligence is used. Hence, the calibrated constitutive model can be used to predict many geotechnical problems. The proposed procedure is validated by comparing the modelled deformations against the real deformations measured during construction of an 8.6m deep soldier pile wall, a four- and five-storey building. The constitutive model used is the Hardening Soil Small Strain model and the structures are modelled in PLAXIS 2D and 3D. The error in most cases does not exceed 1mm.

KEYWORDS: artificial intelligence, pressuremeter, finite elements.

1 INTRODUCTION.

Pressuremeter tests have been used since the 1930's but gained popularity with the Ménard pressuremeter in the 1950's (Mair & Wood, 1987). The general principle of the Ménard pressuremeter test is to insert a cylindrical probe equipped with an expandable flexible membrane into a borehole into the ground. The probe is expanded following a predefined loading program, and the ground responds to the applied load yielding a cavity pressure versus cavity volumetric strain curve. This curve is called a cavity expansion curve and it can be interpreted to derive deformability and strength parameters of the ground. The resulting parameters can be used in many ways, such as to estimate foundation design parameters. The test interpretation relies either on a theoretical analytical background, or on semi-empirical correlations (Lopes, 2022). In practice, the Ménard pressuremeter interpretation is mostly empirical for the reason it will be explained below. In the 1970's Cambridge University researched into a new type of pressuremeters equipped with strain gauges rather than volume gauges which permitted the development of the self-boring pressuremeter and the push-in pressuremeter, these devices allow for the measurement of strains with a resolution of 1 micron ($1x10^{-3}$mm), i.e., about 100 times smaller than the thickness of a sheet of paper. This difference with the Ménard device, which can seem only like a minor detail, makes a huge difference when interpreting the results based on fundamental concepts of soil mechanics. As the soil structure is non homogeneous and the pressuremeter cavity load produces small irregularities along its length (Houlsby & Carter, 1993; Ajalloeian & Yu, 1998) the horizontal displacements measured along the cavity are not all equal, hence, when using a Ménard device only an average horizontal strain along the cavity can be estimated based on the volume admitted, see figure 1. In figure 1, $\Delta_{avg} \neq \Delta_1 \neq \Delta_2 \neq \ldots \Delta_n$.

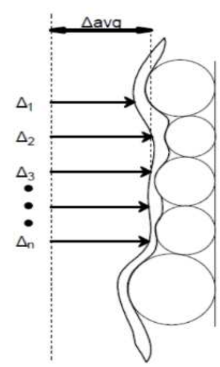

Figure 1. Resolution loss when calculating radial displacement by measuring volume injection.

When using strain gauges the precision estimating the horizontal strains improves dramatically. This phenomenon should not be new to geotechnical engineers as a similar problem occurs when trying to estimate small strain stiffness in a triaxial probe as shown by Jardine (1984). The improvement in resolution implies that the cavity expansion or contraction problem can be approached in a radically different form as previously treated by Ménard and his empirical expressions. In this case an analogy can be traced with the SPT test, which no geotechnical engineer would dare trying to interpret deriving load-deformation curves, as although "feasible" because the load is known and also the displacement, the attempt would surely fail because of resolution problems.

Additionally to the resolution problem the pressuremeter curve presents a second important hindrance when trying to interpret it, which is the complexity of soil behaviour when trying to reduce the boundary value curve measured by the instrument to the single element curve needed for design. Many authors have developed analytical formulations for solving this problem and hence deriving geotechnical properties from the pressuremeter curves (Hughes et al., 1997, Palmer, 1972 and Bolton & Whittle, 1999) but the extent to which analytical expressions can be applied is limited and important simplifications to soil behaviour have to be made in order to resolve the mathematics involved. Others have resorted to numerical formulations (Manassero, 1989; Yu, 1996) improving the accuracy of the soil model but nowadays, only finite element or finite difference models can capture the full complexity of soil behaviour.

The rise of high resolution pressuremeters in recent years and the advent of modern and fast computers and finite element models (FEM) has allowed geotechnical engineers to model the test and back-analyse it in order to obtain the soil properties (Rui & Yin, 2018; Oztoprak & Bolton, 2010; Oztoprak et al., 2018). The authors have been using this procedure for some years with some success (Mella, 2022; Jara, 2023) but the progress of it has been restraint by (1) the long duration of the multiple software iterations needed to obtain a proper curve match and (2) non-uniqueness, i.e., the fact that a single curve can be matched by more than one set of soil properties and only few or one of them relates to real soil behaviour. These two difficulties can be eased by the use of the Artificial Intelligence (AI) software DAARWIN as it will be explained in detail in this article.

In order to assess the applicability of performing a geotechnical characterization by means of modelling a high resolution pressuremeter curve 3 sites that were developed with different structures were monitored during its construction. The first site consisted of an 8.6m deep soldier pile retaining wall, the second a 4-storey high residential building and the third a 5-storey high residential building. Each site was characterised with either 3 or 4 high resolution pressuremeter test at each representative horizon. The construction process was then modelled in either Plaxis 2D or 3D and the soil properties for each horizon were defined by the referred procedure. It will be shown that the Plaxis finite element model calibrated with the referred procedure matches the monitoring with a maximum error of approximately 1mm, hence demonstrating that the AI-aided FEM pressuremeter interpretation delivers an accurate soil characterisation.

2 DAARWIN

DAARWIN is a cloud-based platform based on machine learning genetic algorithms that gathers data, creates connections between design and construction, visualizes construction performance against design analysis, enables 'real-time' back-analysis to enable modifications to design and construction to be made based on actual performance, and better manage risk during underground construction (De Santos 2015).

DAARWIN refines geotechnical design models using data collected from site. It compares the design prediction against the measured response to enable a more accurate understanding and future analysis of the ground and ground-structure interaction behaviours. The resulting back-analysed parameters can be used for further designs, as well as for modifying the existing design and construction sequence through the application of the Observational Method to make them more sustainable, efficient and safer.

Back-analysis is the process where model parameters are changed until an improved match with monitoring data is achieved. Once validated, the model can be extrapolated to make forward predictions of ground and structural behaviour under different conditions. Back-analysis is traditionally performed manually following trial-and-error. With the number of parameters in ground models increasing (especially for more advanced constitutive models), back-analysis typically takes three to six weeks. Accelerating back-analysis to near real-time using DAARWIN has the potential to transform geotechnical practice, and significantly enhances the power of the Observational Method. Because DAARWIN is also a data management platform it can also be a valuable repository of geotechnical information which, if used wisely, can be used to create leaner future designs.

How DAARWIN works:

- Upload the project information into the platform. Numerical models, construction progress monitoring data, images and historical information can be uploaded.
- Analyse multiple design options together with different ground parameter scenarios (from pessimistic, most probable to optimistic) to determine the most optimal design option and the most influential geotechnical parameters.
- Compare the design with the monitoring data to prove that the construction is performing according to design (i.e., confirm the design and construction works are safe and verify the approach).
- Calibrate the numerical models to predict the real ground and ground – structure behaviour.

Although DAARWIN was mainly developed for back-analysing monitoring data of geotechnical structures this work will present its application for interpreting pressuremeter data.

3 SITE DESCRIPTIONS

3.1 *8.6m Soldier pile wall*

The site and monitoring results are described in detail by Jara (2023). The site is located in Concepción, Chile and it is 42m x 43m in plan. It consists of mostly silty sands with one thin silt layer between 10.5m and 11.5m and a thicker silt layer between 14m and 19m. Two CPTu boreholes were pushed and are shown in figure 2. The water table is located at a depth of 5m. One additional borehole was drilled for executing 3 high resolution pressuremeter tests. The cavity was pre-drilled and the 47mm diameter instrument lowered into the hole. Sometimes the pocket did not hold stable and it was necessary to gentle push the instrument into the collapsed ground in order to place it at the desired depth. It has been shown (Hughes & Whittle, 2022) that this insertion disturbance can be dealt with by imposing sufficient deformation during loading and by the unloading of the instrument. The tests were conducted at depths of 2.35m, 5.35m and 10.45m and are shown in figure 3.

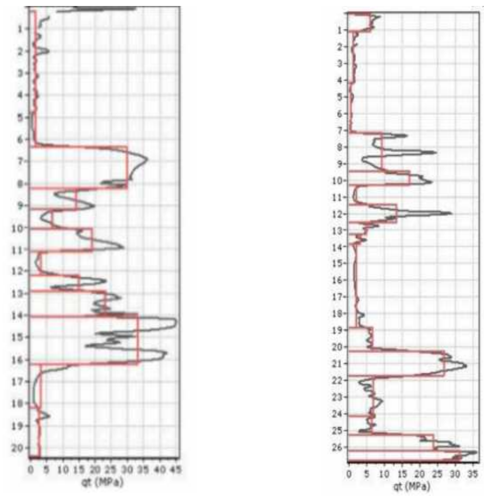

Figure 2. CPTu-01 (left) and CPTU-02 (right), depth in meters.

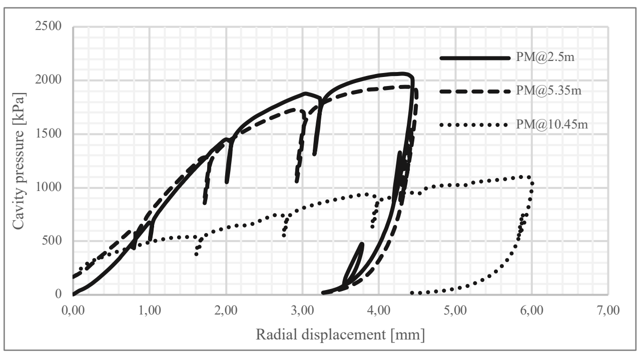

Figure 3. PM Tests at 2.35m, 5.35m and 10.45m

The soldier pile wall consists of H beams W310x38.7 kg/m with a total length of 10.5m, spaced at 1.6m with 2 rows of grouted anchors 127mm in diameter with 4.5m free length and 13.5m and 10.5m bonded length. The timber lagging consisted of dry pine 75mm thick, see figure 4.

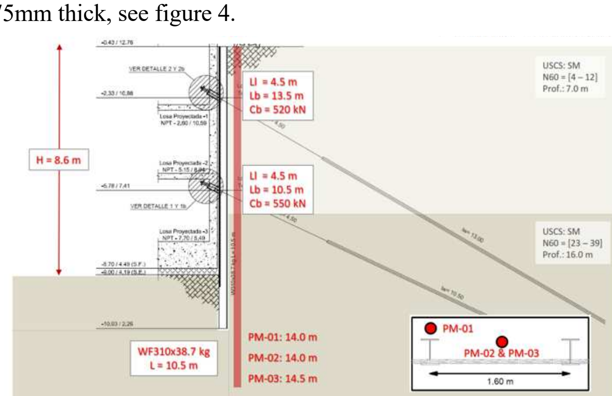

Figure 4. Schematic view of soldier pile wall.

3 inclinometers were installed to a depth of 14m away from the edges to avoid corner effects, see figure 5.

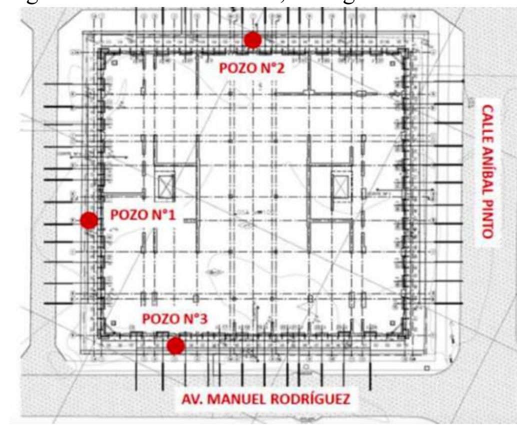

Figure 5. Inclinometers plan location.

A site photograph is shown in figure 6.

Figure 6. Site view.

3.2 *Four-storey building*

The site and monitoring results are described in detail by Mella (2022). The site is located in Chiguayante, Chile and the footprint size of the building is 26m x 15m. The foundations are spread footings. The structure is founded on a 2m thick compacted sandy fill followed by the natural silty sands. One CPTu borehole was pushed and the results are shown in figure 7. The water table is located at a depth of 7m. One borehole was drilled for executing 3 high resolution pressuremeter tests, one in the fill at 1.7m and the others in the silty sand at 3.9m and 6m depth (See figure 8).

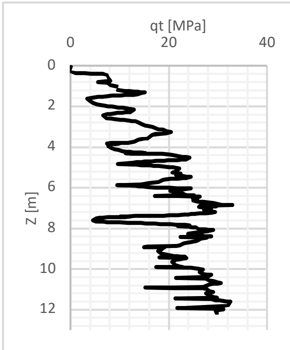

Figure 7. CPTu.

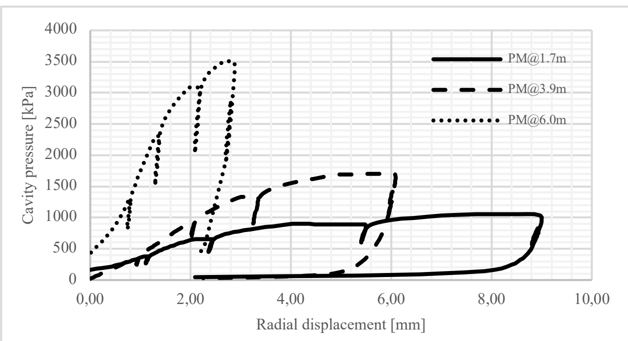

Figure 8. PM Tests at 1.7m, 3.9m and 6.0m.

3.3 *Five-storey building*

The site is located in San Pedro de la Paz, Chile and the footprint building size is 52m x 32m (Mella, 2022). The foundation type corresponds to a slab foundation. The structure is founded on a 5m deep compacted sandy fill overlying the natural soil which correspond to silty sands. Two CPTu boreholes were pushed and are shown in figure 9. The water table is located at a depth of 2m. One borehole was drilled for executing 4 high resolution pressuremeter tests at 2m, 10.5m, 11m and 14.6m, see figure 10, in which the 2m PM is not shown due to reading errors experienced in that test.

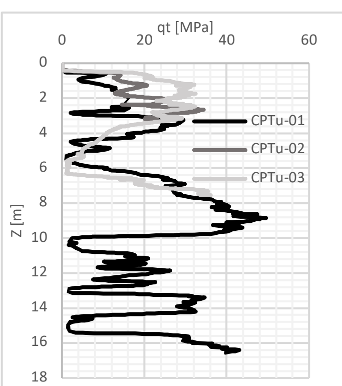

Figure 9. CPTu-01, CPTu-02 and CPTu-03.

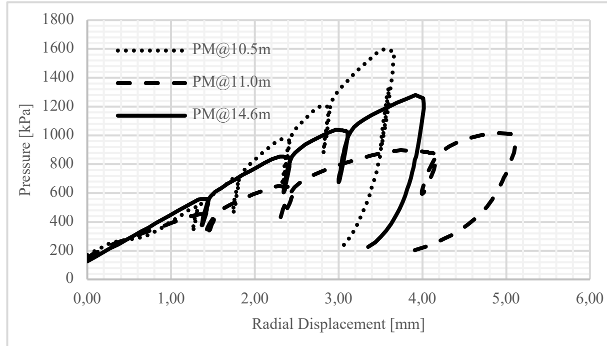

Figure 10. PM Tests at 10.5m, 11.0m and 14.6m

4 PLAXIS MODELLING

4.1 *Soldier pile wall*

A 60m long x 25m deep mesh was used in a plane-strain model in Plaxis 2D to model the wall. The H beam was modelled as a plate element reducing its stiffness in accordance to its spacing. Node to node anchor elements were used to model the anchor free length with an elastic stiffness of 3.5x106 kN/m as embedded beam elements were used to model the anchor grouted length with the following properties:

Table 1. Embedded beam parameters.

E [kN/m^2]	Tskin [kN/m]
2.35E+07	136.4

The soil horizons were modelled as follows:
H1: From 0 to 7.0m
H2: From 7.0m to 10.5m
H3: From 10.5 to 11.5m
H4: From 11.5 to mesh bottom.

Before running DAARWIN's back-analysis sensitivity analyses were carried out in Plaxis varying the angle of shearing resistance of the different strata to very low and very high values. It was observed that even with as low as 28° no considerable amounts of failure points were obtained behind the wall. It was concluded that the given soldier pile wall scheme was mainly controlled by the stiffness properties rather than the soil strength, although in the constitutive model used stiffness and strength are dependent. Notwithstanding, it was decided to leave the angle of shearing resistance out from DAARWIN's iteratives determination process and fix them at expected values defined by the CPTu results. This a priori definition helps the algorithm focusing the search on the parameters that really control the problem and avoiding multiple optima that are sometimes not physically relatable. This is especially true in the case of the Hardening Soil Small Strain (HSS) model as the stiffness also depends from the angle of shearing resistance so one can obtain the same deformation by combining either a low stiffness with a high strength or a high stiffness with a low strength. The angles of shearing resistance fixed for the DAARWIN model are:

H1: ϕ' = 40°
H2: ϕ' = 41°
H3: ϕ' = 28°
H4: ϕ' = 41°

The lateral coefficient of at rest pressure K0 was also fixed at 1.0 for all horizons, as the model used is isotropic and there was no reliable information to use a different value.

The pressuremeters were modelled with a 30m long x 15m deep mesh using an axisymmetric model in Plaxis 2D (figure 11). Simulating the cavity pressure, a uniformly distributed pressure was applied at the test depth at a length of 0.255m which corresponds to the membrane length.

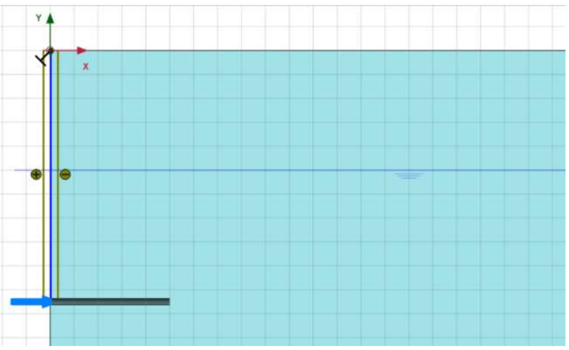

Figure 11. Pressuremeter test model.

In contrast to the wall model, before running DAARWIN, sensitivity analyses showed the dependence on the angle of shearing resistance, hence, in this case, this was a parameter to be determined rather than to be fixed. Hence, for DAARWIN's back analyses, although a high resolution pressuremeter is capable of measuring the shear modulus at small strains G0 (Jara, 2023), it was preferred to fix this value to avoid the same stiffness-strength dependence problem mentioned above. In this manner, the G0 values were fixed at the values determined by the downhole carried out during the CPTu tests.

For both type of analyses, wall and pressuremeter, the relationship recommended by Plaxis was adopted:

$E_{50} = 1.25 \times E_{eod}$

The relationship between E50 and Eur was left free as it will be seen below.
After having back-analysed the pressuremeter tests a wall model was run using these soil parameters. As it can be seen two pressuremeter test were carried out in horizon 1 (PM@2.35m and PM@5.35m) and the third one in horizon 3 (PM@10.45m). As no pressuremeter tests were available for horizons 2 and 4 the same soil parameters obtained with the wall back-analysis were used for these horizons.
Four additional wall models were also implemented in which the properties obtained from PM@2.35m and PM@5.35m were used at horizon 1, 2 and 4.

4.2 *Four-storey building*

A 130m x 70m x 40m deep mesh was used to model the building in Plaxis 3D (figure 12). The spread footing was modelled as a plate element. The transmission of loads to the foundation is through the walls, therefore, the load is modelled linearly distributed along the foundation with a value of q = 17.1 kN/m/storey.

The soil horizons were modelled as follows:

H1: From 0 to 2.0m
H2: From 2.0m to 4.3m
H3: From 4.3 to mesh bottom (40m).

The different soil horizons were characterised by the AI-aided FEM back-analysis of the pressuremeter tests, as described in the previous section.

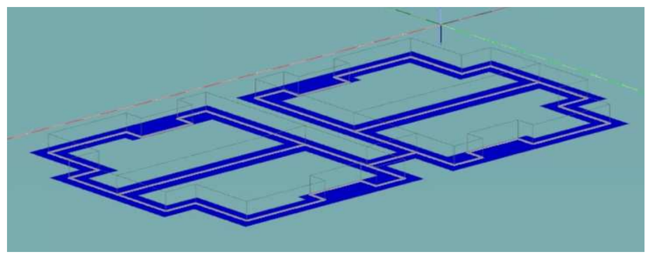

Figure 12. Four-storey building model.

4.3 *Five-storey building*

A 165m x 160m x 50m deep mesh was used to model the building in Plaxis 3D (figure 13). The slab foundation was modeled as a plate element. As in the previous model, the surcharge is modelled as a linear load with a value of q = 24.4 kN/m/storey.

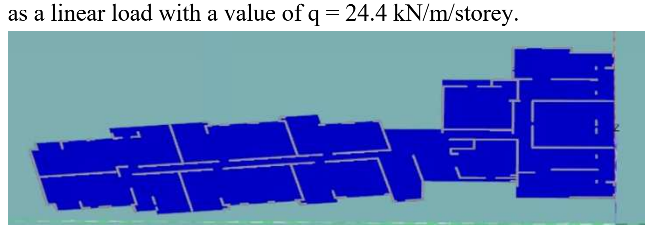

Figure 13. Five-storey building model.

The soil horizons were modelled as follows:

H1: From 0 to 5.0m (PM@1.7m in 4-storey building)
H2: From 5.0m to 9.0m (PM@10.5m)
H3: From 9.0m to 11.0m (PM@11m)
H4: From 11.0 to mesh bottom (PM@14m)

The different soil horizons were characterised by the AI-aided FEM back-analysis of the pressuremeter tests, as described in the previous section. As the 2m PM presented reading problems, for the first horizon the results from the PM at 1.7m from the 4-storey building were used. In this case both horizons correspond to a compacted sandy fill with similar specifications.

5 RESULTS

5.1 *Soldier pile wall*

Table 2 to 5 show the back-analysed parameters for the wall and the pressuremeter for each horizon. The cells in grey denote the parameters have been left free to be determined by DAARWIN. The cells in white denote the parameters have been fixed to the specified value. The reference pressure for all horizons is σ'_3 at the centre of each horizon.

Table 2. Horizon 1 (0m to 7m). Back-analysed parameters.

Parameter	Wall BA	PM BA@2.35m	PM BA@5.35
G0 (MPa)	90	90	90
Eur (MPa)	100	76	39
E50 (MPa)	23	38	14
ϕ ' (°)	40	42	42
$\gamma_{0.7}$	8.65E-04	1.90E-04	1.50E-04
K_0	1.0	4.125	1.2

Table 3. Horizon 2 (7.0m to 10.5m). Back-analysed parameters.

Parameter	Wall BA	PM BA
G0 (MPa)	145	-
Eur (MPa)	56	-
E50 (MPa)	6,5	-
ϕ' (°)	41	-
$\gamma_{0.7}$	2,80E-04	-
K_0	1,0	-

Table 4. Horizon 3 (10,5m to 11,5m). Back-analysed parameters.

Parameter	Wall BA	PM BA@10.45m
G0 (MPa)	85	85,0
Eur (MPa)	61,5	45,0
E50 (MPa)	6,5	8,0
ϕ' (°)	28	30,0
$\gamma_{0.7}$	7,30E-04	5,8E-04
K_0	1,0	1,15

Table 5. Horizon 4 (11,5m to bottom). Back-analysed parameters.

Parameter	Wall BA	PM BA@10.45m
G0 (MPa)	300	-
Eur (MPa)	123.3	-
E50 (MPa)	20	-
ϕ' (°)	41	-
$\gamma_{0.7}$	3.70E-04	-
K_0	1.0	-

Figures 14, 15 and 16 present the back-analyses results for pressuremeters PM@2.5m, PM@5.35m and PM@10.45m.

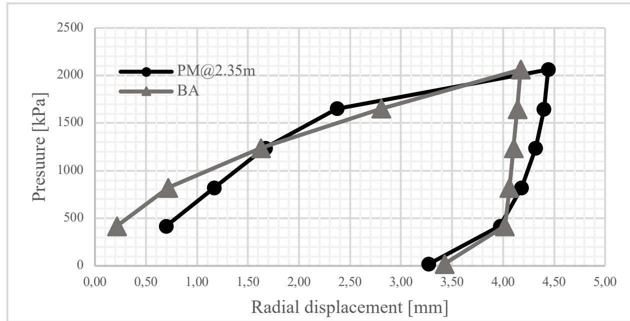

Figure 14. Back-analysed PM@2.35m.

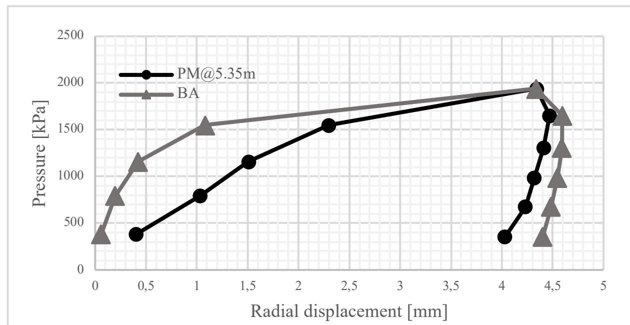

Figure 15. Back-analysed PM@5.35m.

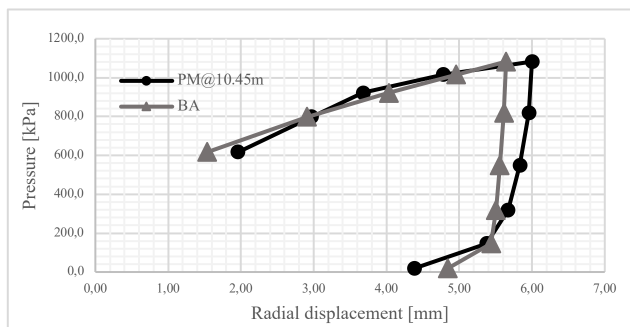

Figure 16. Back-analysed PM@10.45m.

As constitutive models are calibrated as a whole it can be misleading to compare percentage differences between each parameter. Instead of comparing for each horizon the difference between each parameter for the wall and pressuremeter back analyses it is more fruitful to compare the horizontal displacements obtained for each model. Figure 17, 18 and 19 present the horizontal displacements measured by the most representative inclinometer and the different wall models. The results obtained by Jara (2023) with the same data is also shown. In that work the author carried out back-analyses for each pressuremeter test adjusting the parameters manually in Plaxis. According to the author a period of 3 weeks was needed to obtain the results. For this work, a period of 2 working days -16 hours – was recorded. The time saved by DAARWIN is salient and the improvement in prediction is approximately threefold. In Figure 16, it can be seen that the maximum prediction error by back-analysing the pressuremeters is approximately 1mm, a notable feat for geotechnical deformation predictions. As there were no pressuremeter test conducted at horizons H2 and H4 the soil parameters for these horizons are taken from the Wall BA. Figure 17 presents the results using the back-analysed results for PM@2.35m and PM@5.35m at horizons H1 and H2, the back - analysed results for PM@10.45m for H3 and the Wall BA for H4. Figure 18 presents the results using the back-analysed results for PM@2.35m and PM@5.35m at horizons H1, H2 and H4 and the back-analysed results for PM@10.45m for H3. Hence, even without having characterised horizons H2 and H4 with pressuremeters, the soil parameters determined for horizon H1 are good enough for obtaining a deformation prediction with a maximal error less than 2mm.

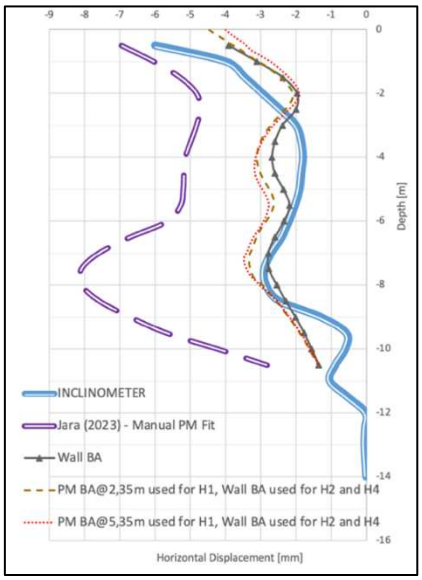

Figure 17. Horizontal Displacements. Wall BA for H2 and H4.

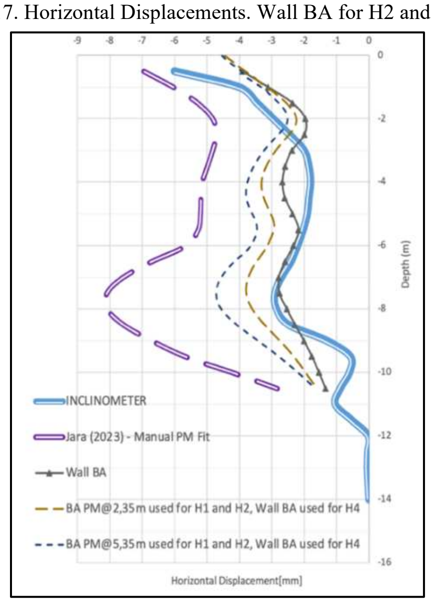

Figure 18. Horizontal Displacements. Wall BA for H4.

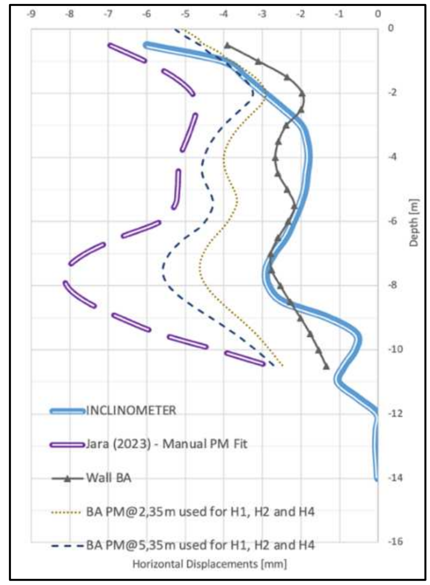

Figure 19. Horizontal Displacements. PM used for all horizons.

It is important to highlight that although the Wall BA curve represents a better fit of the actual wall movements, this curve corresponds to the best fit that a machine learning algorithm can obtain using Plaxis after having been fed with the actual soil movements, i.e., this curve does not represent a prediction. In contrast, the PM BA curves could have been obtained before the actual wall construction had taken place.

5.2 *Four-storey building*

Table 6 show the back-analysed parameters for the pressuremeters for each horizon. The cells in white denote the parameters have been left free to be determined by DAARWIN. The cells in grey denote the parameters have been fixed to the specified value. The reference pressure for all horizons is σ'$_3$ at the centre of each horizon.

Table 6. Horizons. Back-analysed parameters.

Parameter	PM@1.7m	PM@3.9m	PM@6.0m
G0 (MPa)	72.8	106.9	216.1
Eur (MPa)	61.0	53.0	156.0
E50 (MPa)	4.0	18.0	78.0
$\gamma_{0.7}$	6.2E-4	4.0E-5	4.0E-5
ϕ' (°)	37	34	41
K_0	4.80	3.88	4.43

Figure 20 presents the back-analysed pressuremeter curve performed by DAARWIN. For conciseness, only 1 curve will be shown here.

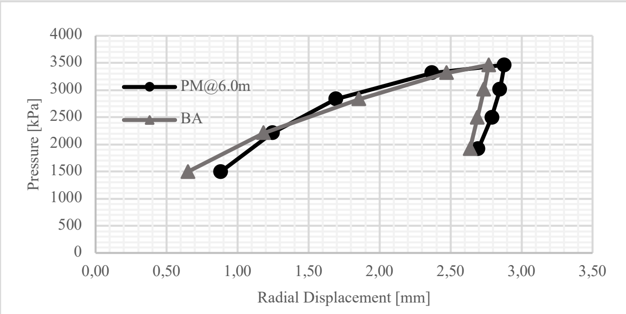

Figure 20. Back-analysed PM@6.0m.

Figure 21 compares the Plaxis 3D computed accumulated settlements against the measured ones for each loading phase and for a representative foundation point. As it can be seen the prediction is very good, with an error of approximately 0.5mm.

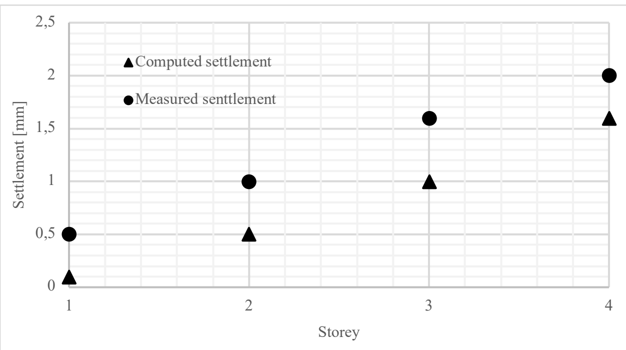

Figure 21. Computed vs measured cumulative settlements.

5.2 *Five-storey building*

Table 7 show the back-analysed parameters for the pressuremeters for each horizon. The cells in white denote the parameters have been left free to be determined by DAARWIN. The cells in grey denote the parameters have been fixed to the specified value. The reference pressure for all horizons is σ'$_3$ at the centre of each horizon.

Table 7. Horizons. Back-analysed parameters.

parameter	PM@10.5m	PM@11.0m	PM@14.6m
G0 (MPa)	332.9	264.9	333.6
Eur (MPa)	60.0	88.0	14.0
E50 (MPa)	28.0	23.0	51.0
$\gamma_{0.7}$	1.0E-6	7.0E-6	2.0E-6
ϕ' (°)	37	34	39
K_0	2.65	1.03	2.03

Figure 22 presents the back-analysed pressuremeter curve performed by DAARWIN. For conciseness, only 1 curve will be shown here.

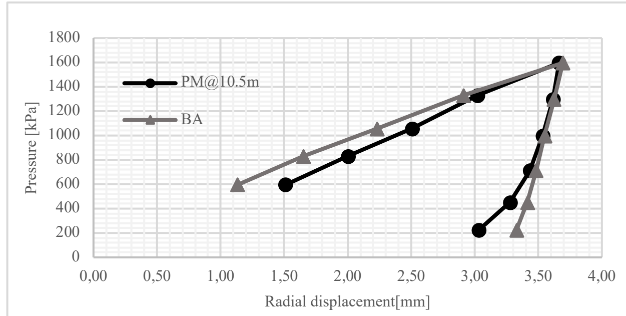

Figure 22. Back-analysed PM@10.5m.

Figure 23 compares the Plaxis 3D computed accumulated settlements against the measured ones for each loading phase and for a representative foundation point. As it can be seen the prediction is remarkable, with a maximum error of about 1mm.

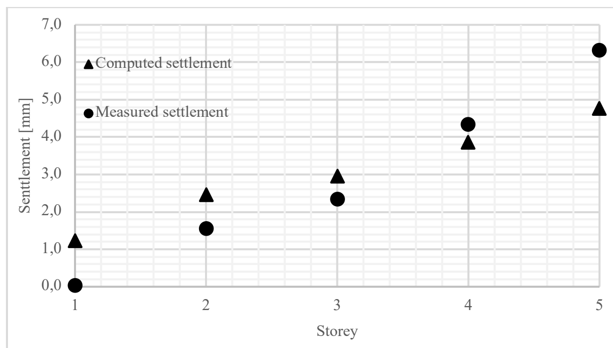

Figure 23. Computed vs measured cumulative settlements.

5.3 *General Results*

An interesting result obtained with the proposed procedure is the determination of Ko. Values ranging from 4 to close to 1 have been obtained with increasing depth. The value of Ko determined by the procedure might depend on the degree of disturbance made during the insertion process so further analyses will have to be carried out in order to bring more light into this difficult and important aspect of soil behaviour.

A general Hughes et al (1977) loading analysis for sand would give much lower ϕ' values than the ones reported in this article and very different to the ones obtained by the CPTu. For example, for H-1 in the case of the soldier pile wall a Hughes et al (1977) analysis gives ϕ' = 32° in contrast with ϕ' = 42° given by the pressuremeter-FEM analysis and ϕ' = 40° given by the CPTu. The reason for this huge difference is because the analytical method ignores the elastic deformations in the plastic deforming region and it was shown by Yu (1990) that neglecting elastic strains in the plastic zone tends to give a softer pressuremeter response and therefore underestimates the measured angle of friction. This is of great importance as it shows that adopting more realistic soil models when interpreting pressuremeters can have enormous consequences for the values of the soil parameters obtained.

The angle of shearing resistance values obtained by the pressuremeter closely match the CPT defined values. CPT-derived ϕ' values for a silty sand can be considered reliable in this case as the calibration chambers in which CPT-ϕ' values are determined closely resemble the silty sand deposit conditions - no boundary effects, homogeneous grain size, regular geology, etc. Notwithstanding, with the proposed approach the ϕ'-pressuremeter values are not determined by correlations, they are determined by strict fundamental soil mechanics principles. This would imply that the approach can be applied to more complex materials such as residual soils, highly weathered rock as the Chilean Maicillo, gravels, or even materials that would hardly classify as soil as the salty rocks encountered for mining the nowadays in fashion Lithium. The authors have tested these materials with the referred pressuremeter and have obtained insightful results which will be discussed elsewhere.

These are all materials in which unaltered samples are hard to obtain and transport into a laboratory to test in a triaxial test, for example. Even if the materials were to be sampled in a disturbed fashion, accepting the loss of natural structure, their maximum particle size to sample size ratio would normally imply the use of uncommercial laboratory apparatuses - recent research suggests this ratio is much larger than the factor of 10 normally used and can reach a factor as high as 20 (Cantor & Ovalle, 2023). As pointed out by Hughes and Whittle (2022), the pressuremeter mobilises a much larger volume than traditional laboratory tests - 50 times more than a commercial triaxial probe, hence, solving this issue for an important range of materials, see Figure 24.

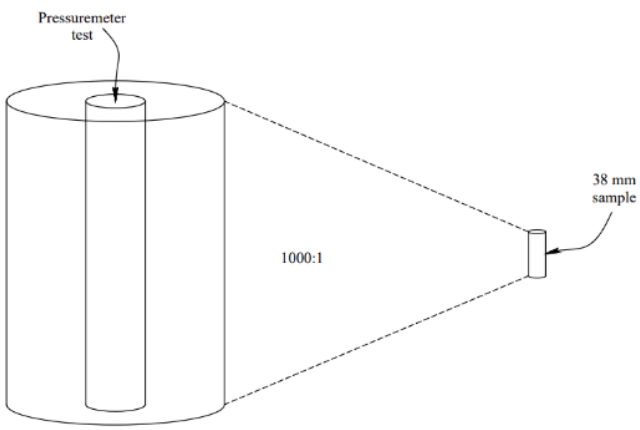

Figure 24. A pressuremeter mobilises a 50 times larger volume than a 38mm diameter triaxial sample (Hughes and Whittle, 2022).

6 CONCLUSIONS

In order to assess the applicability of performing a geotechnical characterisation by means of numerically modelling a high resolution pressuremeter curve, 3 sites that were developed with different structures were monitored during its construction. The first site consisted of an 8.6m deep soldier pile retaining wall, the second a 4-storey high residential building and the third a 5-storey high residential building. Each site was characterised with either 3 or 4 high resolution pressuremeter test at each representative horizon. The construction process was modelled in either Plaxis 2D or 3D and the soil properties for each horizon were defined by back-analysing the pressuremeter curve with an AI software called DAARWIN that uses PLAXIS. It was shown that the Plaxis finite element model calibrated with the referred procedure matched the monitoring with a maximum error of approximately 1mm, hence demonstrating that the pressuremeter-derived soil properties accurately represent the ground behaviour and improving the soil characterisation that would have been obtained by traditional pressuremeter interpretation methods.

Horizontal deformations were predicted in the case of the soldier pile wall and vertical deformations were predicted in both buildings' cases, hence predicting 2 different stress paths with the radial horizontal stress path measured by the pressuremeter. This would also confirm the wide field of applications appropriate for pressuremeters and reduce concerns regarding soil anisotropy, at least in the tested geology.

The proposed method is in principle suitable for the geotechnical characterisation of many types of problems: dams, slopes, piles, foundations, etc. and many geotechnical materials: residual soils, heavily weathered rock, gravel, clays, etc. as the pressuremeter is an in-situ test that can be pre-drilled for its installation.

A notable feature of using pressuremeters in conjunction with finite element models is that constitutive models are calibrated as a whole with all soil parameters being properly interconnected to reproduce the full stress-strain response, something that cannot be achieved by conventional SPT or CPTu tests. The simplifications historically used for solving the mathematics involved in reducing the boundary value problem to a single element curve can be overridden, hence adopting much more sophisticated and realistic soil models and consequently obtaining more accurate geotechnical properties.

7 ACKNOWLEDGEMENTS

The authors would like to thank Cristian de Santos CEO at SAALG Geomechanics, Berta Solá and Laia Gelonch Geotechnical Engineers at SAALG Geomechanics for their support and advice using DAARWIN and pointing them in the right direction to obtain the results presented in this article. For the continuous guidance in carrying out tests as well as with hardware support the authors would also like to thank Simon Baxter and Robert Whittle from Cambridge In-Situ.

8 REFERENCES

Ajalloeian, R., & Yu, H. (1998). Chamber studies of the effects of pressuremeter geometry on test results in sand. Géotechnique/Geotechnique, 48(5), 621-636. https://doi.org/10.1680/geot.1998.48.5.621

Bolton, M. D., & Whittle, R. W. (1999). A non-linear elastic/perfectly plastic analysis for plane strain undrained expansion tests. Géotechnique/Geotechnique, 49(1), 133-141. https://doi.org/10.1680/geot.1999.49.1.133

Cantor, D., & Ovalle, C. (2023). Sample size effects on the critical state shear strength of granular materials with varied gradation and the role of column-like local structures. Géotechnique/Geotechnique, 1-12. https://doi.org/10.1680/jgeot.23.00032

De Santos C. Backanalysis Methodology Based on Multiple Optimization Techniques for Geotechnical Problems. Ph.D. thesis. Universitat Politècnica de Catalunya – BarcelonaTECH. 2015.

Houlsby, G. T., & Carter, J. (1993). The effects of pressuremeter geometry on the results of tests in clay. Géotechnique/Geotechnique, 43(4), 567-576. https://doi.org/10.1680/geot.1993.43.4.567

Hughes, J. M. O., Wroth, C. P., & Windle, D. (1977). Pressuremeter tests in sands. Géotechnique/Geotechnique, 27(4), 455-477. https://doi.org/10.1680/geot.1977.27.4.455

Hughes, J. P., & Whittle, R. R. (2022). High Resolution Pressuremeters and Geotechnical Engineering. En CRC Press eBooks. https://doi.org/10.1201/9781003200680

Jara, M. (2023). Modelamiento Numérico de un Muro Berlinés Caracterizado Mediante Datos de Presiómetro en Descarga. [Tesis de pre – grado para optar a título de Ingeniero Civil. Universidad de Concepción].

Jardine, R. J., Symes, M. J., & Burland, J. B. (1984). The Measurement of soil stiffness in the triaxial apparatus. Géotechnique/Geotechnique, 34(3), 323-340. https://doi.org/10.1680/geot.1984.34.3.323

Lopes A. 2022. Louis Ménard and the pressuremeter test. Comité Francais de la Mécaniqe des Sols. Accesed on 27th Abril 2024. https://www.cfmssols.org/sites/default/files/timecapsule/2%20Pressiometre%20et%20Menard/EN%20rapport%20pressiom%C3%A8tre%20M%C3%A9nard.pdf

Mair, R. J., & Wood, D. M. (1987). Pressuremeter testing: Methods and Interpretation. Butterworth-Heinemann.

Manassero, M. (1989). Stress-strain relationships from drained self-boring pressuremeter tests in sands. Géotechnique/Geotechnique, 39(2), 293-307. https://doi.org/10.1680/geot.1989.39.2.293

Mella, M. (2022). Análisis crítico de parámetros de deformación para la estimación de asentamientos en edificios en Concepción. [Tesis de pre – grado para optar a título de Ingeniero Civil. Universidad de Concepción].

Oztoprak, S. & Bolton, M. (2010). Parameter calibration of modified hyperbolic model for sands using pressuremeter test data. International Symposium on Deformation Characteristics of Geomaterials, September 1-3, 2010, Seoul, Korea.

Oztoprak, S., Sargin, S., Uyar H., & Bozbey I. (2018). Modeling of pressuremeter test to characterize the sands. Geomechanics an Engineering, Vol. 14, No 6 (2018) 509-517. https://doi.org/10.12989/gae.2018.14.6.6.509

Palmer, A. (1972). Undrained plane-strain expansion of a cylindrical cavity in clay: a simple interpretation of the pressuremeter test. Géotechnique/Geotechnique, 22(3), 451-457. https://doi.org/10.1680/geot.1972.22.3.451

Rui, Y., & Yin, M. (2018). Interpretation of pressuremeter test by finite-element method. Proceedings Of The Institution Of Civil Engineers. Geotechnical Engineering/Proceedings Of ICE. Geotechnical Engineering, 171(2), 121-132. https://doi.org/10.1680/jgeen.17.00032

Yu, H.S. (1990). Cavity Expansion Theory and its Application to the Analysis of Pressuremeters. DPhil Thesis, Oxford University.

Yu, H.S. (1996). Interpretation of pressuremeter unloading tests in sands. Géotechnique/Geotechnique, 46(1), 17-31. https://doi.org/10.1680/geot.1996.46.1.17.